

# INTERACTION OF MACRO-PARTICLES WITH LHC PROTON BEAM

F. Zimmermann, M. Giovannozzi, CERN, Switzerland; A. Xagkoni, NTU Athens, Greece

## Abstract

We study the interaction of macro-particles residing inside the LHC vacuum chamber, e.g. soot or thermal-insulation fragments, with the circulating LHC proton beam. The coupled equations governing the motion and charging rate of metallic or dielectric micron-size macro-particles are solved numerically to determine the time spent by such “dust” particles close to the path of the beam as well as the resulting proton-beam losses, which could lead to a quench of superconducting magnets and, thereby, to a premature beam abort.

## INTRODUCTION

Dust trapping is a well known phenomenon in electron storage rings, e.g. [1, 2, 3, 4]. where a positively charged “dust” or macro-particle is attracted by the electric field of the negatively charged beam, getting further ionized as it approaches the beam, which leads to its “trapping” close to the beam center and to a concomitant drop in beam lifetime. For sufficiently high beam-current density — typically at Ampère-level beam currents for  $e^+e^-$  factories — trapped macro-particles are heated under the continuous bombardment from the beam particles so much that they ultimately melt and explode [4].

During an incident in September 2008 some portions of the LHC beam pipe were contaminated with insulation parts, soot and metallic macro-particles [5]. In the case of a proton beam, as in the LHC, the force between a positively charged macro-particle and the beam is repulsive so that dust trapping is not expected. In fact it has never been observed for protons beams. Therefore, for the LHC, long-term trapping of dust particles by the beam is not a concern. However, the initial charge state of a macro-particle can be positive as well as negative (or neutral), and for the LHC the question is of interest if such negatively charged (or neutral) macro-particles, initially moving towards the beam, could give rise to locally enhanced beam losses that might disrupt LHC operation.

Charged macro-particles are subject to electric forces of the beam field, to electric image forces at the vacuum-chamber walls, and to gravity. For various reasons they can start to move, e.g. due to eddy currents induced by a varying strong magnetic field [6].

In the LHC, if a moving macro-particle comes close to the beam the resulting enhanced local beam losses could lead to quenches of superconducting (SC) magnets. On the other hand, as it approaches the beam the macro-particle will also be ionized by beam protons passing through it,

and become positively charged, whereupon it will be expelled from the vicinity of the beam.

In this paper we discuss two aspects of the interaction between macro-particles and the LHC proton beam, namely the possibility that macro-particles can be picked up from the bottom of the vacuum chamber by the electric field of the beam, and the magnitude of beam losses expected at the moment of a dust particle’s closest approach to the center of the beam.

## MACRO-PARTICLE DYNAMICS

A charged macro-particle moves under the influence of primarily three forces: (1) electric beam force, (2) electric image force, and (3) gravity. Its charging rate is determined by ionizing collisions of beam particles together with secondary electron escape from the charged macro-particle. Since the heavy macro-particle moves slowly, the bunched nature of the beam is unimportant, and for computing the motion of the macro-particle it is sufficient to consider the average electric field of the beam.

Further, making the simplifying assumptions of a transversely round beam, with Gaussian shape and horizontal or vertical rms size  $\sigma$ , and of a round macro-particle with mass  $A$ , in units of proton masses  $m_p$ , density  $\rho$  and radius  $R$ , the various forces give rise to the following transverse acceleration rates

$$\vec{a}_{\text{el., beam}} = \frac{2N_p Q r_p c^2}{AC} \left(1 - e^{-\frac{x^2+y^2}{2\sigma^2}}\right) \frac{\vec{r}}{r^2}, \quad (1)$$

$$\vec{a}_{\text{image}} = \frac{Q^2 r_p c^2}{A \left(\frac{b^2}{r} - r\right)^2} \frac{\vec{r}}{r}, \quad (2)$$

$$\vec{a}_{\text{grav}} = -g \begin{pmatrix} 0 \\ 1 \end{pmatrix}, \quad (3)$$

and to the equation of motion

$$\ddot{\vec{r}} = \vec{a}_{\text{el., beam}} + \vec{a}_{\text{image}} + \vec{a}_{\text{grav}}, \quad (4)$$

where  $r = \sqrt{x^2 + y^2}$  denotes the radial distance from the beam center,  $\vec{r} = (x, y)$  the (unnormalized) radial distance vector,  $y$  the vertical position with respect to the center of the chamber ( $y > 0$  refers to positions above the center),  $x$  the horizontal coordinate,  $b$  the radius of the vacuum chamber, assumed to be round,  $C$  the circumference of the storage ring,  $N_p$  the total number of protons in the beam,  $c$  the speed of light,  $r_p$  the classical proton radius (about  $1.5 \times 10^{-18}$  m),  $Q$  the charge of the macro-particle in units of the electron charge, and  $g$  the acceleration from gravity ( $9.81 \text{ m/s}^2$ ). The total acceleration is the sum of the above expressions.

Table 1: Beam parameters

protons/beam	$N_p$	$2808 \times 1.15 \times 10^{11}$
rms beam size	$\sigma$	0.3 mm
circumference	$C$	26659 m

The additional acceleration from the magnetic Lorentz force, of order  $evB/(m_p A)$ , can in first approximation be neglected for the typical speed  $v$  of the macro-particles despite the high magnetic field  $B \approx 8.3$  T of the LHC dipole magnets at top energy. For example, even with a macro-particle speed as high as 1 m/s, the magnetic force is about 200 times smaller than the electric force from the beam at the chamber wall.

Under some assumptions ( $Q \gg 1$ ) the charging rate is determined from the distribution of high-energy secondary electrons with energy high enough to escape from the electric potential of the dust particle [2],

$$\dot{Q} \approx -\frac{4\pi}{3} f_{\text{rev}} 1000 N_A r_e \frac{N_p R^4}{2\sigma^2 Q} \left(\frac{\rho}{\text{kg}}\right) e^{-\frac{x^2+y^2}{2\sigma^2}}, \quad (5)$$

where  $m_e$  signifies the electron mass,  $N_A$  Avogadro's number,  $f_{\text{rev}}$  the beam revolution frequency, and  $r_e$  the classical electron radius, and  $Z_{\text{atom}} \approx A_{\text{atom}}/2$  was used. The radius  $R$  of the macro-particle is related to its mass  $A$  via

$$R \approx (3A/(4\pi(\rho/\text{kg}) 1000 N_A))^{1/3}. \quad (6)$$

We can solve the coupled nonlinear equations of motion (4) and (5), together with (1), (2), and (3), using the Mathematica [7] function *NDSolve*.

Table 1 lists typical beam parameters for the LHC design. Properties of a few candidate ‘‘dust’’ materials are summarized in Table 2. In the following we consider the example of a macro-particle made from aluminium, representing e.g. a piece of multilayer insulation foil.

Figure 1 depicts the charging rate (5) as a function of distance from the center of the beam. The probability of its charging, say over a time interval of 1 s, is negligibly small if the macro-particle is more than  $10\sigma$  away from the beam.

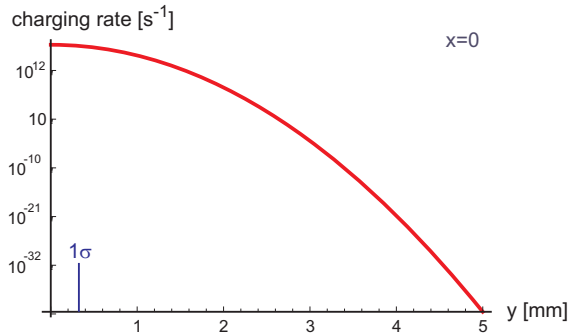


Figure 1: Charging rate  $\dot{Q}$  for a macro-particle with mass  $A = 10^{13}$  and initial charge  $Q = -1$  as a function of vertical distance  $y$  from the beam center, at  $x = 0$ .

Table 2: Some properties of carbon, aluminium, and copper

material	$A_{\text{atom}}$	$Z_{\text{atom}}$	$\rho$ [kg/m <sup>3</sup> ]	$\sigma_{\text{int}}$ [barn]
carbon	12	6	2000	0.126
aluminium	27	13	2700	0.420
copper	64	29	9000	0.553

Figure 2 presents the total acceleration experienced by a particle with a single negative charge which is located at the chamber wall either above or below the beam. The figure demonstrates that for the nominal beam current macro-particles heavier than about  $10^{11}$  proton masses can fall into the beam from above, but that the nominal beam current is too low to pick up any charged particles from the bottom of the beam pipe whichever their mass. For low macro-particle masses this is prevented by the image-charge force, for high masses by gravity. At a beam current ten times higher than nominal a small window opens up at intermediate mass values between  $10^{10}$  and  $10^{11}$  proton masses where macro-particles could then be lifted by the electric field of the beam.

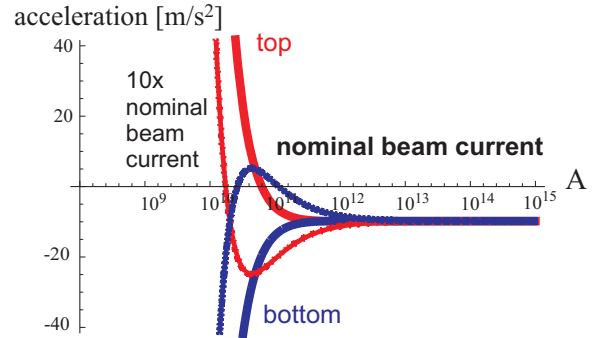


Figure 2: Total vertical acceleration at the upper (red) or lower (dark blue) chamber wall due to the beam force, image force and gravity as a function of the mass of a singly charged [ $Q=-1$ ] dust particle, for the nominal LHC beam current (bold) and for ten times this current (thin).

Figure 3 shows some example trajectories and charge evolutions of macro-particles of different mass, initially moving towards the beam. As the particle comes close to the beam it quickly charges up and gets repelled. The final charge of the particle is roughly proportional to its mass.

## BEAM LOSS RATE

Local beam losses arise from hard nuclear interactions with the nuclei of the macro-particle. Interaction cross sections for some dust materials are compiled in Table 2. The local loss rate is estimated as

$$\dot{N}_p = \frac{\sigma_{\text{int}} N_p c}{2\pi\sigma^2 C} \frac{A}{A_{\text{atom}}} e^{-\frac{x^2+y^2}{2\sigma^2}}. \quad (7)$$

This loss rate can be compared with the quench limit for SC magnets. The latter has been simulated by FLUKA to

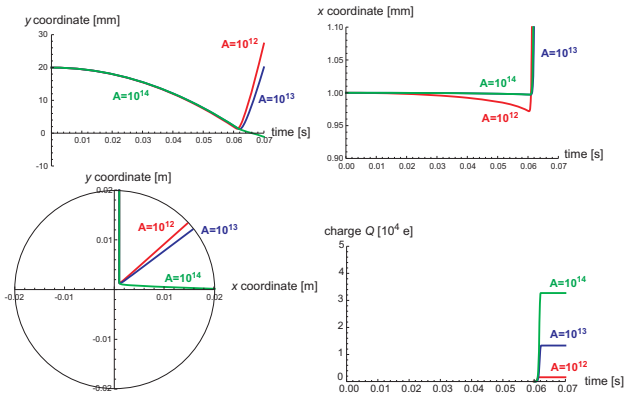


Figure 3: Vertical and horizontal position of macro-particles with three different masses, as indicated, and initial charge  $Q = -1$ , launched at  $x = +1$  mm above the beam, as a function of time (top); the same trajectories in the  $x - y$  plane, and associated charge evolutions (bottom).

correspond to a value of  $1-2 \times 10^7$  protons lost per second at top energy, and to about 15 times more at injection, for continuous losses, or by a sudden transient loss of  $10^7$  protons at top energy [8, 9]. Figure 4 shows the beam-loss rate due to a particle with  $A = 10^{13}$  as a function of the particle position. The time-dependent proton-beam loss rates expected for the three macro-particle trajectories of Fig. 3 are presented in Fig. 5. The magnitude of the peak loss rate, at the turning point of the macro-particle trajectory, is about 10 protons per seconds and lasts only about 1 ms, so that both the continuous and the instantaneous losses remain far below the corresponding magnet quench thresholds.

From (5), we can define a charging cross section  $\sigma_{\text{charging}} = \pi r_e A_{\text{atom}} R / |Q|$ , in analogy to the nuclear interaction cross section  $\sigma_{\text{int}}$  of (7). The initial charging cross section is of order Gbarn or about 9 orders of magnitude larger than the nuclear cross section, which explains why the macro-particles rapidly charge in the periphery of the beam without causing any serious beam loss.

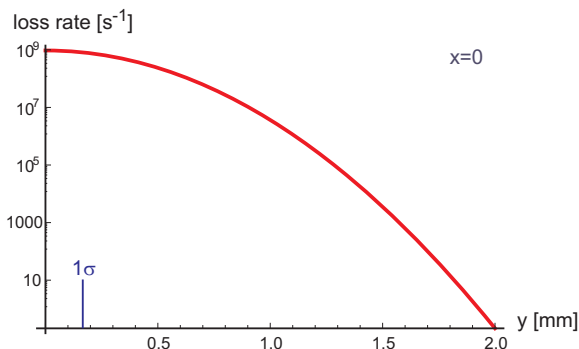


Figure 4: Beam loss rate for a macro-particle with mass  $A = 10^{13}$  as a function of vertical distance  $y$  from the beam center, at  $x = 0$ .

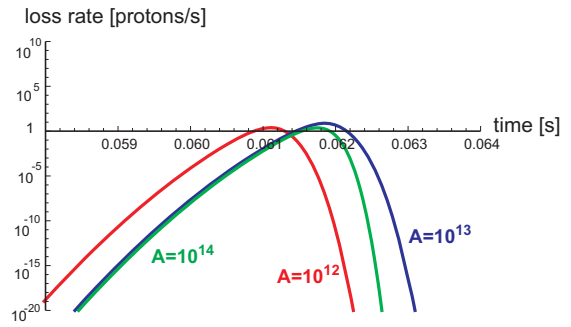


Figure 5: Beam loss rate for the three macro-particle trajectories of Fig. 3.

## CONCLUSIONS

We have developed computing tools for modeling the interaction of charged macro-particles with the LHC proton beam. Example calculations demonstrate that the LHC beam, even at nominal current, is not able to pick up (round) charged dust particles from the bottom of the vacuum chamber. However, sufficiently heavy dust particles could fall into the beam from above, or they could start to move towards the beam as a result of mechanical vibration or of eddy currents induced while the magnetic field is ramped. We have examined trajectories and charge states of such macro-particles, and we have calculated the associated beam-loss rates. The latter reach their maximum values at the trajectory turning points, when the macro-particles acquire a positive charge and start to be repelled. In all cases the maximum beam loss stays far below the value at which quenches of superconducting magnets are expected. The underlying reason is the much larger magnitude of the “charging cross section” compared with the nuclear cross section. Future work may extend this discussion to other macro-particle shapes, e.g. “needles”.

## REFERENCES

- [1] C. Sagan, “Mass and Charge Measurements of Trapped Dust in the CESR Storage Ring,” NIM A330 371 (1993).
- [2] F. Zimmermann, “Trapped Dust in HERA and DORIS,” DESY HERA 93-08 (1993)
- [3] F. Zimmermann, “Trapped Dust in HERA and Prospects for PEP-II,” PEP-II AP Note No.: 8-94 (1994)
- [4] F. Zimmermann, J.T. Seeman, M. Zolotarev, W. Stoeffl, “Trapped Macroparticles in Electron Storage Rings,” IEEE PAC’95 Dallas (1995).
- [5] V. Baglin, “Can we optimise the cleanup process further?,” Proc. LHC Performance Workshop Chamonix 2010, 25-29 January 2010.
- [6] F. Caspers, private communication (2008).
- [7] Wolfram Research, Mathematica 7.
- [8] M. Brugger, F. Cerutti, A. Ferrari, V. Vlachoudis, “FLUKA Estimations Concerning Obstacles in the LHC Magnets,” CERN-AB-Note-2007-018 ATB (2007).
- [9] The FLUKA Team, “Summary of FLUKA Estimations for Obstacles in the LHC Magnets,” private communication by G. Arduini, 24.02.2009